HHS Public Access

Author manuscript

Arthritis Rheumatol. Author manuscript; available in PMC 2018 June 01.

Published in final edited form as:

Arthritis Rheumatol. 2017 June ; 69(6): 1187–1193. doi:10.1002/art.40047.

Treatment of TNF-Tg Mice with Anti-TNF Restores Lymphatic Contraction, Repairs Lymphatic Vessels, and May Increase Monocyte/Macrophage Egress

Echoe M. Bouta, PhD[a,b], **Igor Kuzin, PhD**[c], **Karen de Mesy Bentley, MS**[a,i], **Ronald W. Wood, PhD**[d,e], **Homaira Rahimi, MD**[a,f], **Rui-Cheng Ji, MD, PhD**[g], **Christopher T. Ritchlin, MD, MPH**[a,h], **Andrea Bottaro, PhD**[c], **Lianping Xing, BM, PhD**[a,i], and **Edward M. Schwarz, PhD**[a,b,e,h,i]

[a]Center for Musculoskeletal Research, University of Rochester School of Medicine and Dentistry, Rochester, NY, USA

[b]Department of Biomedical Engineering, University of Rochester School of Medicine and Dentistry, Rochester, NY, USA

[c]Department of Biomedical Sciences, Cooper Medical School of Rowan University, Camden, NJ, USA

[d]Department of Obstetrics and Gynecology, University of Rochester School of Medicine and Dentistry, Rochester, NY, USA

[e]Department of Urology, University of Rochester School of Medicine and Dentistry, Rochester, NY, USA

[f]Department of Pediatrics, University of Rochester School of Medicine and Dentistry, Rochester, NY, USA

[g]Faculty of Welfare and Health Science, Oita University, Oita, Japan

[h]Division of Allergy, Immunology, Rheumatology, Department of Medicine, University of Rochester School of Medicine and Dentistry, Rochester, NY, USA

[i]Department of Pathology and Laboratory Medicine, University of Rochester School of Medicine and Dentistry, Rochester, NY, USA

Abstract

Corresponding author: Dr. Edward M. Schwarz, The Center for Musculoskeletal Research, University of Rochester Medical Center, 601 Elmwood Avenue, Box 665, Rochester, NY 14642, Phone: 585-275-3063, Fax 585-275-1121, Edward_Schwarz@URMC.Rochester.edu.

Financial Disclosure

Anti-TNF therapy was provided by Janssen Pharmaceuticals Inc.

AUTHOR CONTRIBUTIONS

All authors were involved in drafting the article or revising it critically for important intellectual content, and all authors approved the final version to be published. Dr. Schwarz had full access to all of the data in the study and takes responsibility for the integrity of the data and the accuracy of the data analysis.

Study conception and design: Bouta, Kuzin, Xing, Bottaro, Ritchlin, Schwarz

Acquisition of data: Bouta, Kuzin, Ji

Analysis and interpretation of data: Bouta, Kuzin, de Mesy-Bentley, Wood, Rahimi, Ji, Ritchlin, Bottaro, Xing, Schwarz

Background—Recent studies have demonstrated that there is an inverse relationship between lymphatic egress and inflammatory arthritis in affected joints. As a model, TNF-transgenic (TNF-Tg) mice develop advanced arthritis following draining lymph node collapse, and loss of lymphatic contractions downstream of inflamed joints. As it is unknown if these lymphatic deficits are reversible, we tested the hypothesis that anti-TNF therapy reduces advanced inflammatory-erosive arthritis, associated with restoration of lymphatic contractions, repair of damaged lymphatic vessels, and evidence of increased monocyte egress.

Methods—TNF-Tg mice with advanced arthritis and collapsed popliteal lymph nodes (PLN) were treated with anti-TNF monoclonal antibody (10 mg/kg weekly) or placebo for 6-weeks, and effects on knee synovitis, efferent lymphatic vessel ultrastructure and function, and PLN cellularity were assessed by ultrasound, histology, transmission electron microscopy (TEM), near infrared indocyanine green (NIR-ICG) imaging, and flow cytometry, respectively.

Results—Anti-TNF therapy significantly decreased synovitis ~5-fold ($p<0.05$ vs. placebo), restored lymphatic contractions, and significantly increased PLN monocytes/macrophages ~2-fold ($p<0.05$ vs. placebo). TEM demonstrated large activated macrophages attached to damaged lymphatic endothelium in mice with early arthritis, extensively damaged lymphatic vessels in placebo-treated mice with advanced arthritis, and rolling leukocytes in repaired lymphatic vessels in mice responsive to anti-TNF therapy.

Conclusion—These findings support the concept that anti-TNF therapy ameliorates inflammatory-erosive arthritis, in part, via restoration of lymphatic vessel contractions and potential enhancement of inflammatory cell egress.

Keywords

Rheumatoid Arthritis; anti-TNF Drugs; Mouse Models; RA

INTRODUCTION

Despite the establishment of tumor necrosis factor inhibitors (anti-TNF) as a standard of care for rheumatoid arthritis (RA), the mechanisms by which they ameliorate synovitis in inflamed joints remains incompletely understood. Specifically, how an anti-TNF agent reduces synovial macrophage numbers independent of apoptosis (1, 2), and alters monocyte influx into the synovium (3), remains an open question. One possible explanation is that TNF inhibition increases efflux of macrophages/monocytes from the synovium, which is supported by studies demonstrating that anti-TNF increases lymphangiogenesis in murine inflammatory arthritis and RA patients (4, 5). However, anti-TNF induced cellular egress from flaring joints has yet to be formally demonstrated.

Previously, we demonstrated that arthritic progression in knee joints of TNF-transgenic (Tg) mice is paralleled by dramatic changes in the draining lymph nodes (6–8). These longitudinal imaging studies combining contrast enhanced (CE) MRI of the synovium and popliteal lymph node (PLN) (6), with quantitation of lymphatic drainage via near infrared (NIR) imaging of an injected dye (indocyanine green, ICG) (9), demonstrated that prior to detectable synovial hyperplasia in the knee, the adjacent PLN expands due to increased lymphangiogenesis, lymphatic fluid accumulation, $CD11b^+$ macrophage infiltration, and the

expansion of a unique subset of $CD23^{+}/CD21^{hi}$ B cells in inflamed nodes (B-in) (5, 9–14). This asymptomatic “expansion” phase is followed by a sudden “collapse” of the PLN, which is identified by CE-MRI or power doppler imaging of the PLN (6, 15). This collapse, which occurs at variable time intervals in ~80% of TNF-Tg mice, is associated with B-in translocation from the follicles to LYVE-1^{+} lymphatic vessels of the paracortical sinuses, a reduction in volume and increase in PLN fluid pressure (6, 8, 16). Thereafter, lymphatic drainage declines significantly due to loss of intrisic lymphatic contractions and passive flow (8, 10, 13, 17). It was also demonstrated that B-cell depletion therapy (BCDT) with anti-CD20 antibodies ameliorated knee flare afferent to collapsed PLN by “clearing” the LN sinuses, and restoring passive lymphatic flow in the absence of lymphatic contractions (8). However, whether agents that target the underlying etiology of inflammatory arthritis can restore lymphatic vessel contractions during the “collapsed” phase of the disease remains an open question. To this end, we evaluated anti-TNF effects on advanced knee arthritis in TNF-Tg mice to determine if lymphatic contraction can be restored.

MATERIALS AND METHODS

Animals and treatment

All animal research was conducted on IACUC approved protocols. TNF-Tg mice (3647 line) (18) were originally acquired from Dr. G. Kollias, and are maintained as heterozygotes in a C57BL/6 background. For all imaging, mice were anesthetized with 1.5–2% isoflurane. TNF-Tg male mice (8–10 months old) with collapsed PLN were treated with anti-TNF or non-specific IgG1 isotype placebo control monoclonal antibodies (CNTO12 and CNTO151, respectively, 10 mg/kg weekly intraperitoneally, Janssen, Spring House, PA, USA) as previously described (6).

Contrast enhancement MRI acquisition and analysis

MRI scans and analysis were performed as described previously (6, 10, 11). Briefly, TNF-Tg mice were anesthetized and the knee and ankle were inserted into a customized coil and were imaged in a 3T Siemens Trio (Siemens MedicalSolutions, Erlangen, Germany). After a pre-contrast scan, 0.5 mL/kg gadolinium-diethylenetriamine pentaacetic acid (Gd-DTPA) contrast agent (Omniscan, Amersham Health, Oslo, Norway) was injected into the orbital venous plexus. The post-contrast scan was started 5 minutes after injection to allow for circulation of Gd-DTPA.

Histology

For histology, knees were harvested and fixed in 10% neutral buffered formalin. The joints were then decalcified in 14% ethylenediaminetetraacetic acid at room temperature for 21 days. Joints were then embedded in paraffin and cut into 5 μm sections. Sections were deparaffinized and stained for alcian blue hematoxylin/orange G (ABH/OG), tartrate-resistant acid phosphatase (TRAP), or F4/80 (AbD Serotec, Raleigh, NC, USA) as described previously (6, 10, 11).

Power Doppler ultrasound (PD-US)

The PLN of TNF-Tg mice were phenotyped as collapsed using PD-US as previously described (15). PD-US was also performed on the knee joints as previously described (19). Each joint was imaged with a high-resolution small-animal ultrasound system (VisualSonics 770, Toronto, Ontario, Canada) using a 704b scanhead.

Near infrared indocyanine imaging

Mice were placed on a heated surface (Indus Instruments, Webster, TX, USA), hair was removed with a depilatory cream and the mouse footpad was injected with 10 μl of 0.1% ICG (Akorn, Lake Forest, Illinois, USA) as previously described (20). The imaging system was composed of a lens (Zoom 7000, Navitar, Rochester, NY, USA), ICG filter set (Semrock, Lake Forest, IL, USA) and camera (Prosilica GT1380, Allied Vision Technologies, Exton, PA, USA). ICG was excited with a tungsten halogen bulb (IT 9596ER, Illumination Technologies, Inc., Syracuse, NY, USA) through a ring illuminator (Schott, Elmsford, NY, USA). Imaging settings and recordings were accomplished through a custom built LabVIEW program (National Instruments, Austin, TX, USA). Real time NIR imaging was performed for 60 minutes after ICG injection into the footpad to quantify the lymphatic contraction frequency, and mice were imaged 24 hours later to quantify percent ICG clearance as previously described (20).

Flow cytometry

Single cell suspensions were prepared from lymph nodes by mechanical disruption and stained with a mixture of fluorochrome-conjugated monoclonal antibodies: CD3 (clone 17A2), CD11b (M1/70), MHC II (M5/114.15.2) and Gr1 (RB6-8C5) from Biolegend, CD19 (1D3) and CD11c (clone HL3) from BD Pharmingen and F4/80 (BM8) from eBioscience (San Diego, CA, USA) as previously described (13). All the samples were stained for dead cell exclusion using live/dead fixable violet dead cell stain kit (Invitrogen, Grand Island, NY, USA) and fixed in 1% formaldehyde before running on the instrument. Samples were run on a 12-color LSRII cytometer (BD Pharmingen, San Jose, CA, USA) and analyzed using FlowJo software (Tree Star Inc., Ashland, OR, USA).

Transmission Electron Microscopy

The afferent lymphatic vessel to the PLN was identified by injecting Evan’s blue in the footpad and was then excised and immersion fixed at 4°C using a combination fixative of 2.5% glutaraldehyde and 4.0% paraformaldehyde in 0.1 M sodium cacodylate buffer for 24 hours. The specimens were rinsed in 0.1M sodium cacodylate buffer and post-fixed with buffered 1% osmium tetroxide. The tissue was dehydrated in a graded series of ethanol to 100%, transitioned into propylene oxide, infiltrated with EPON/Araldite epoxy resin, followed by embedment in fresh resin and polymerization for 2 days at 60°C. To identify the lymphatic vessel in the specimen, the epoxy embedded block was cut serially into one micron slices and stained with toluidine blue. Then the lymphatic vessel was trimmed of excess surrounding tissue and thin sectioned at 70 nm using a diamond knife and ultramicrotome. The thin sections were placed onto formvar/carbon slot nickel grids carbon coated nickel grids, and stained with uranyl acetate and lead citrate. A Hitachi 7650

Transmission Electron Microscope with a Gatan 11 megapixel Erlangshen digital camera was used to image the grids.

Statistical analysis

A Mann-Whitney or t-test was used to test for significance if it was not normally distributed or normally distributed, respectively. Normality was tested for using a Shapiro-Wilk normality test. Longitudinal studies were tested with two-way ANOVA with multiple comparisons corrected for by controlling the False Discovery Rate or Bonferroni post-test. Significance was considered $p<0.05$.

RESULTS

Consistent with our prior studies (10), anti-TNF therapy significantly decreased knee synovial volume versus placebo as assessed by CE-MRI (Supplemental Figure 1). Anti-TNF therapy reduced joint inflammation, bone erosion and osteoclast numbers as assessed by histology (Supplemental Figures 2A–D). Furthermore, immunohistochemistry demonstrated that numbers of $F4/80^+$ macrophages in knee synovium were markedly reduced in anti-TNF treated mice versus placebo (Supplemental Figures 2E & F). We also performed PD volume measurements in the knee joint space as an additional assessment of synovial vascularity and inflammation. After six weeks of treatment, higher PD signal (red) was obvious in the placebo group, compared to the anti-TNF treatment group (Supplemental Figures 2G & H). Longitudinally, US showed a dramatic and continual increase in PD volume in the placebo group, while anti-TNF prevented an increase in joint inflammation (Supplemental Figure 2I).

Longitudinal NIR-ICG imaging demonstrated a remarkable increase in lymphatic transport following anti-TNF treatment, compared to placebo mice that displayed low or absent ICG uptake at 6-weeks (Figure 1A–G). Quantification of lymphatic contraction frequency confirmed that the anti-TNF drug effects were in part due to active transport (Figure 1C and F), which resulted in increased lymphatic clearance (Figure 1G). Remarkably, anti-TNF treated mice showed consistent, regular lymphatic contractions that were significantly increased versus placebo, and equivalent to WT (~2 contractions/min), similar to previous studies (8). Moreover, this is the first demonstration that lymphatic contractions can be recovered after PLN collapse in this model.

To further dissect the mechanisms of action of anti-TNF therapy, we assessed drug effects on cellular compositions in the PLN by flow cytometry. The results showed that the increased cellular egress from inflamed joints following anti-TNF treatment was accompanied by higher total cell numbers in collapsed PLN of TNF-Tg mice (Table 1). Although our cellular subset analysis displayed trends suggesting increased B-cells and T-cells, the only PLN populations that were significantly changed by anti-TNF therapy was a 2.1-fold increase in the ($CD3^-CD19^-CD11b^+$) monocytes/macrophages and a 2.9-fold increase in granulocytes ($CD3^-CD19^-CD11b^+CD11c^-F4/80^-Gr1^+$). Taken together these findings support a model in which anti-TNF therapy ameliorates synovitis potentially by enhancing cellular egress from the joint via active lymphatic transport through the draining lymph nodes.

To corroborate our finding of anti-TNF induced monocyte/macrophage egress, we performed TEM on the lymphatic vessels afferent to PLN. Wild-type lymphatic vessels showed intact lymphatic endothelial and muscle cells (Figure 2A and B) with lumens void of cells. Vessels afferent to expanding PLN showed initial, and what appeared as weak, luminal attachment of large (>5 μm) macrophages to the endothelial cells (Figure 2C), while vessels afferent to collapsed PLN show these activated macrophages firmly attached to the endothelial cells, indicated by the increased surface area of macrophage attachment (Figure 2D). TEM images of lymphatic vessels from placebo-treated mice displayed extensive tissue destruction as evidenced by large vacuoles in endothelial cells and degenerated muscle cells (Figure 2E). Remarkably, mice with collapsed PLN treated with anti-TNF therapy showed evidence of restored cellular egress, as TEM revealed small (<2 μm) leukocytes with a rolling cell morphology on the luminal endothelium (red asterisks in Figure 2F). In particular, we did not observe cytoplasmic vacuoles in endothelial cells, a finding associated with damaged lymphatic vessels, providing additional support to explain the recovery of lymphatic contraction (15).

DISCUSSION

Advances in drug development over the last two decades provide an array of treatment options in RA (21, 22). Despite this progress, major unmet clinical needs remain for a significant proportion of RA patients (~40%) who are partial responders, or prove refractory to all current therapies including anti-TNF. There is also a larger group of RA patients who suffer from periodic arthritic flare. Thus, new therapeutic strategies are needed, which requires formal elucidation of current drug mechanism of action. To this end, we have focused on lymphatic changes during arthritic progression and flare (6, 10, 13, 20, 23) and the effects of interventions that specifically target lymphatic contractions, whose physiologic importance in supporting lymphatic drainage and subsequent onset of lymphedema have been established in preclinical and clinical studies (24, 25).

It is well known that monocytes/macrophages (type 1 synoviocytes) are the most abundant cell type in RA inflamed synovium, and that these cells are a major source of inflammatory mediators and catabolic factors in pannus tissue (26). Moreover, results from RA trials with various drug therapies have shown that clinical efficacy directly correlates with an observed decrease in $CD68^+$ synovial sublining macrophages (27, 28). Many studies have addressed the mechanisms responsible for the reduction of RA macrophage/monocytes in response to anti-TNF, but the findings have been inconclusive and contradictory. For example, while anti-TNF-induced apoptosis of synoviocytes in RA has been reported (29), other studies failed to observe these effects (1, 2). Other reports demonstrated that anti-TNF therapy reduces generation of osteoclasts and bone erosion (30). In contrast, we find that anti-TNF decreases macrophage/monocyte numbers in the joint by increasing lymphatic transport and potentially cell egress from inflamed joints. These findings are further supported by previous studies demonstrating that anti-TNF therapy increased lymphangiogenesis both in a murine model and in RA patients (4). Consistently, our data demonstrate that reduction in joint inflammation (Supplemental Figure 1 and 2) is accompanied by an increase in lymphatic contraction frequency and lymphatic clearance (Figure 1), and a significant increase in the number of $CD11b^+$ cells in the draining lymph node (Table 1). Previously, we have shown

that CD11b$^+$ cells migrate in lymphatic vessels afferent to expanding PLN, and are immobile within these lymphatic vessel during the PLN collapsed phase (8). Therefore, the best explanation for the concomitant decrease in myeloid synoviocytes with increased CD11b$^+$ cells in the PLN after 6-weeks of anti-TNF therapy is increased cell egress through lymphatics, as shown by the rolling leukocytes in lymphatic vessels (Figure 2F). However, important points that remain to be addressed in our study include the possibility that CD11b$^+$ cells enter the PLN through high endothelial venules and a potential increase in T-cells and B-cells. Therefore, formal histology studies to determine the temporal and spatial increases in distinct myeloid and lymphocytic populations in the PLN following anti-TNF therapy are planned as a future direction. It may also be possible to assess increased lymphatic clearance following anti-TNF treatment of RA patients using new NIR-ICG imaging methods (23).

In addition to our anti-TNF studies in TNF-Tg mice described here and elsewhere (6, 10, 11), we have also assessed the effects of anti-CD20 in this RA model (13, 20). Although head-to-head efficacy studies have yet to be performed, there were several general findings that highlight distinct drug mechanisms of action on joint inflammation and lymphatic clearance. The first is that anti-TNF therapy ameliorates arthritis in both ankle and knee joints, while anti-CD20 and genetic B-cell depletion only affects knee arthritis (20). This may be due to anti-TNF effects on both tenosynovitis that drives ankle arthritis in this model (31), and knee flare triggered by the loss of lymphatic drainage (Supplemental Figure 1), while anti-CD20 only affects the latter (13, 20). Secondly, anti-CD20 efficacy appears to be due to “unclogging” of lymphatic vessels to restore passive lymphatic flow, as evidenced by a dramatic increase PLN contrast enhancement on CE-MRI and loss of B-in cells without lymphatic contractions (20), while anti-TNF targets the underling etiology in this model to decrease inflammation and restore lymphatic contractions (Figure 1) without decreasing PLN B-cell numbers (Table 1).

In summary, these data show that in a murine model of arthritis, TNF inhibition is followed by increased lymphatic drainage from the joint providing a possible clearance mechanism for inflammatory cells. More importantly, we demonstrate for the first time that a therapeutic agent can restore steady normal lymphatic contractions subsequent to arthritic flare associated with collapsed draining lymph nodes and the loss of lymphatic contraction. Thus, drugs specifically designed to facilitate lymphatic vessel repair and return of lymphatic contractions remain intriguing and novel treatments for additional exploration.

Supplementary Material

Refer to Web version on PubMed Central for supplementary material.

Acknowledgments

Anti-TNF therapy was provided by Janssen Research and Development LLC. We thank Pat Weber for her technical assistance with CE-MRI, Gayle Schneider for her technical assistance thin sectioning for TEM, and Sarah Mack and Kathy Maltby for their technical assistance with histology. This work was supported by research grants from the National Institutes of Health PHS awards (T32 AR053459; K08 AR067885; R01s AR069000, AR048697 and AR056702; P01 AI078907 and P30 AR069655).

References

1. Smeets TJ, Kraan MC, van Loon ME, Tak PP. Tumor necrosis factor alpha blockade reduces the synovial cell infiltrate early after initiation of treatment, but apparently not by induction of apoptosis in synovial tissue. Arthritis Rheum. 2003; 48(8):2155–62. [PubMed: 12905468]
2. Wijbrandts CA, Remans PH, Klarenbeek PL, Wouters D, van den Bergh Weerman MA, Smeets TJ, et al. Analysis of apoptosis in peripheral blood and synovial tissue very early after initiation of infliximab treatment in rheumatoid arthritis patients. Arthritis Rheum. 2008; 58(11):3330–9. [PubMed: 18975323]
3. Herenius MM, Thurlings RM, Wijbrandts CA, Bennink RJ, Dohmen SE, Voermans C, et al. Monocyte migration to the synovium in rheumatoid arthritis patients treated with adalimumab. Ann Rheum Dis. 2011; 70(6):1160–2. [PubMed: 21345816]
4. Polzer K, Baeten D, Soleiman A, Distler J, Gerlag DM, Tak PP, et al. Tumour necrosis factor blockade increases lymphangiogenesis in murine and human arthritic joints. Ann Rheum Dis. 2008; 67(11):1610–6. [PubMed: 18174217]
5. Zhang Q, Lu Y, Proulx S, Guo R, Yao Z, Schwarz EM, et al. Increased lymphangiogenesis in joints of mice with inflammatory arthritis. Arthritis Res Ther. 2007; 9(6):R118. [PubMed: 17997858]
6. Proulx ST, Kwok E, You Z, Papuga MO, Beck CA, Shealy DJ, et al. Longitudinal assessment of synovial, lymph node, and bone volumes in inflammatory arthritis in mice by in vivo magnetic resonance imaging and microfocal computed tomography. Arthritis Rheum. 2007; 56(12):4024–37. [PubMed: 18050199]
7. Li J, Zhou Q, Wood R, Kuzin I, Bottaro A, Ritchlin CT, Xing L, Schwarz EM. CD23+/CD21hi B cell translocation and ipsilateral lymph node collapse is associated with asymmetric arthritic flare in TNF-Tg mice. Arthritis Res Ther. 2011; 13(4):R138. [PubMed: 21884592]
8. Li J, Ju Y, Bouta EM, Xing L, Wood RW, Kuzin I, et al. Efficacy of B cell depletion therapy for murine joint arthritis flare is associated with increased lymphatic flow. Arthritis Rheum. 2013; 65(1):130–8. [PubMed: 23002006]
9. Zhou Q, Wood R, Schwarz EM, Wang YJ, Xing L. Near-infrared lymphatic imaging demonstrates the dynamics of lymph flow and lymphangiogenesis during the acute versus chronic phases of arthritis in mice. Arthritis Rheum. 2010; 62(7):1881–9. [PubMed: 20309866]
10. Proulx ST, Kwok E, You Z, Beck CA, Shealy DJ, Ritchlin CT, et al. MRI and quantification of draining lymph node function in inflammatory arthritis. Ann N Y Acad Sci. 2007; 1117:106–23. [PubMed: 17646265]
11. Proulx ST, Kwok E, You Z, Papuga MO, Beck CA, Shealy DJ, et al. Elucidating bone marrow edema and myelopoiesis in murine arthritis using contrast-enhanced magnetic resonance imaging. Arthritis Rheum. 2008; 58(7):2019–29. [PubMed: 18576355]
12. Guo R, Zhou Q, Proulx ST, Wood R, Ji RC, Ritchlin CT, et al. Inhibition of lymphangiogenesis and lymphatic drainage via vascular endothelial growth factor receptor 3 blockade increases the severity of inflammation in a mouse model of chronic inflammatory arthritis. Arthritis Rheum. 2009; 60(9):2666–76. [PubMed: 19714652]
13. Li J, Kuzin I, Moshkani S, Proulx ST, Xing L, Skrombolas D, et al. Expanded CD23(+)/CD21(hi) B cells in inflamed lymph nodes are associated with the onset of inflammatory-erosive arthritis in TNF-transgenic mice and are targets of anti-CD20 therapy. J Immunol. 2010; 184(11):6142–50. [PubMed: 20435928]
14. Kuzin II, Kates SL, Ju Y, Zhang L, Rahimi H, Wojciechowski W, et al. Increased numbers of CD23(+) CD21(hi) Bin-like B cells in human reactive and rheumatoid arthritis lymph nodes. Eur J Immunol. 2016; 46(7):1752–7. [PubMed: 27105894]
15. Bouta EM, Ju Y, Rahimi H, de Mesy-Bentley KL, Wood RW, Xing L, et al. Power Doppler Ultrasound Phenotyping of Expanding versus Collapsed Popliteal Lymph Nodes in Murine Inflammatory Arthritis. PLoS One. 2013; 8(9):e73766. [PubMed: 24040061]
16. Bouta EM, Wood RW, Brown EB, Rahimi H, Ritchlin CT, Schwarz EM. In vivo Quantification of Lymph Viscosity and Pressure in Lymphatic Vessels and Draining Lymph Nodes of Arthritic Joints in Mice. J Physiol. 2014; 592(Pt 6):1213–23. [PubMed: 24421350]

17. Li J, Zhou Q, Wood R, Kuzin I, Bottaro A, Ritchlin C, et al. CD23+/CD21hi B cell translocation and ipsilateral lymph node collapse is associated with asymmetric arthritic flare in TNF-Tg mice. Arthritis Res Ther. 2011; 13(4):R138. [PubMed: 21884592]
18. Keffer J, Probert L, Cazlaris H, Georgopoulos S, Kaslaris E, Kioussis D, et al. Transgenic mice expressing human tumour necrosis factor: a predictive genetic model of arthritis. EMBO J. 1991; 10(13):4025–31. [PubMed: 1721867]
19. Bouta EM, Banik PD, Wood RW, Rahimi H, Ritchlin CT, Thiele RG, et al. Validation of Power Doppler Versus Contrast Enhanced Magnetic Resonance Imaging Quantification of Joint Inflammation in Murine Inflammatory Arthritis. J Bone Miner Res. 2014
20. Li J, Ju Y, Bouta EM, Xing L, Wood RW, Kuzin I, et al. Efficacy of B cell depletion therapy for murine joint arthritis flare is associated with increased lymphatic flow. Arthritis Rheum. 2012; 65(1):130–8.
21. Smolen JS, Landewe R, Breedveld FC, Dougados M, Emery P, Gaujoux-Viala C, et al. EULAR recommendations for the management of rheumatoid arthritis with synthetic and biological disease-modifying antirheumatic drugs. Ann Rheum Dis. 2010; 69(6):964–75. [PubMed: 20444750]
22. Keystone EC, Smolen J, van Riel P. Developing an effective treatment algorithm for rheumatoid arthritis. Rheumatology (Oxford). 2012; 51(Suppl 5):v48–54. [PubMed: 22718927]
23. Rahimi H, Bell R, Bouta EM, Wood RW, Xing L, Ritchlin CT, et al. Lymphatic imaging to assess rheumatoid flare: mechanistic insights and biomarker potential. Arthritis Res Ther. 2016; 18:194. [PubMed: 27586634]
24. Zawieja DC. Contractile physiology of lymphatics. Lymphat Res Biol. 2009; 7(2):87–96. [PubMed: 19534632]
25. Mallick A, Bodenham AR. Disorders of the lymph circulation: their relevance to anaesthesia and intensive care. Br J Anaesth. 2003; 91(2):265–72. [PubMed: 12878626]
26. Firestein GS. Evolving concepts of rheumatoid arthritis. Nature. 2003; 423(6937):356–61. [PubMed: 12748655]
27. Zwerina J, Hayer S, Tohidast-Akrad M, Bergmeister H, Redlich K, Feige U, et al. Single and combined inhibition of tumor necrosis factor, interleukin-1, and RANKL pathways in tumor necrosis factor-induced arthritis: effects on synovial inflammation, bone erosion, and cartilage destruction. Arthritis Rheum. 2004; 50(1):277–90. [PubMed: 14730626]
28. Mould AW, Tonks ID, Cahill MM, Pettit AR, Thomas R, Hayward NK, et al. Vegfb gene knockout mice display reduced pathology and synovial angiogenesis in both antigen-induced and collagen-induced models of arthritis. Arthritis Rheum. 2003; 48(9):2660–9. [PubMed: 13130487]
29. Catrina AI, Trollmo C, af Klint E, Engstrom M, Lampa J, Hermansson Y, et al. Evidence that anti-tumor necrosis factor therapy with both etanercept and infliximab induces apoptosis in macrophages, but not lymphocytes, in rheumatoid arthritis joints: extended report. Arthritis Rheum. 2005; 52(1):61–72. [PubMed: 15641091]
30. Binder NB, Puchner A, Niederreiter B, Hayer S, Leiss H, Bluml S, et al. Tumor necrosis factor-inhibiting therapy preferentially targets bone destruction but not synovial inflammation in a tumor necrosis factor-driven model of rheumatoid arthritis. Arthritis Rheum. 2013; 65(3):608–17. [PubMed: 23280418]
31. Hayer S, Redlich K, Korb A, Hermann S, Smolen J, Schett G. Tenosynovitis and osteoclast formation as the initial preclinical changes in a murine model of inflammatory arthritis. Arthritis Rheum. 2007; 56(1):79–88. [PubMed: 17195210]

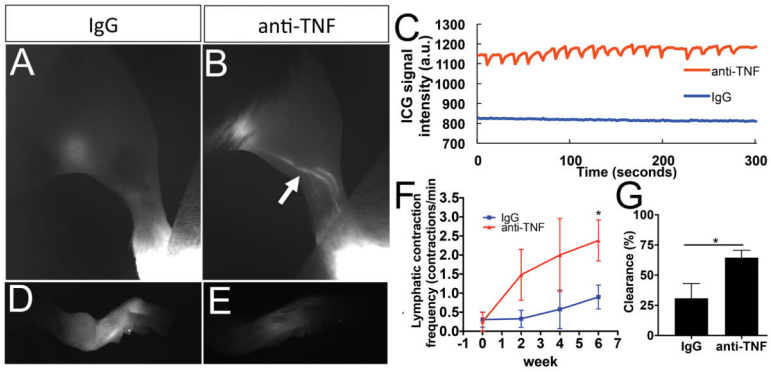

Figure 1. Anti-TNF therapy restores lymphatic contraction in TNF-Tg mice with advanced arthritis

Male TNF-Tg mice (n=6) were randomized to anti-TNF or IgG placebo treatment following PD-US confirmation of PLN collapse and baseline NIR-ICG imaging to confirm loss of lymphatic contractions. Following commencement of therapy, the mice underwent NIR-ICG imaging every 2-weeks for 6-weeks to assess recovery of lymphatic contractions. Representative NIR images of the lower limb obtained 1 hour after ICG injection (A, B), and of the injected foot 24 hours later (D, E), after 6-weeks of therapy are shown. Note that ICG-filled lymphatic vessels were most apparent in the anti-TNF treated mice (arrow in B). Representative examples of the raw signal intensity data used to quantify lymphatic contraction are shown to illustrate the recovery observed at 6-weeks in anti-TNF treated mice versus the absence of contractions in placebo (C). Note that residual ICG was greater in the feet of placebo treated mice (D vs. E). The quantified lymphatic contraction frequency (F, two-way ANOVA with multiple comparisons corrected for by controlling the False Discovery Rate showed a treatment effect with $p=0.01$), and % ICG clearance at 6-weeks (G) are presented as the mean ± SEM (*$p<0.05$ via Mann-Whitney test).

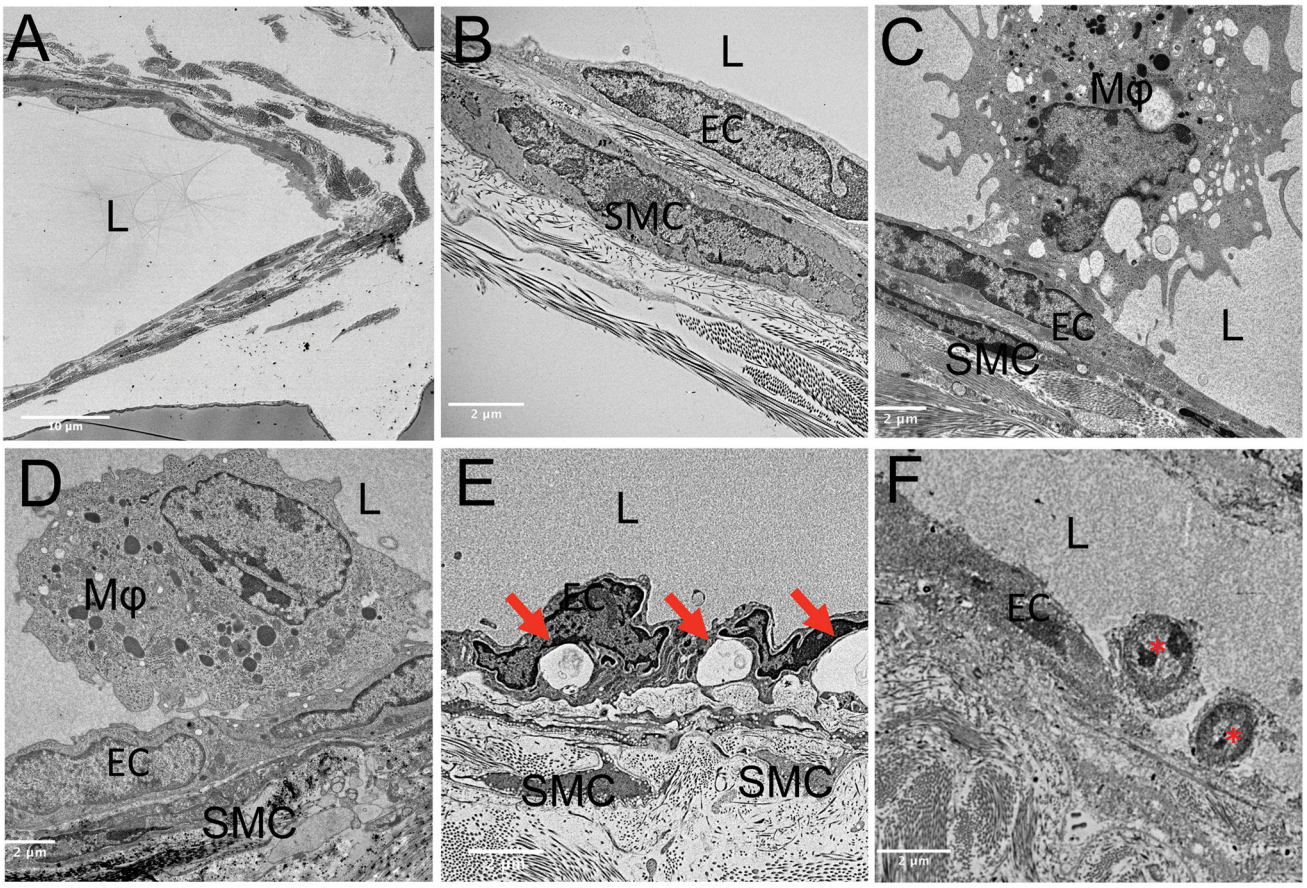

Figure 2. Ultrastructural evidence of lymphatic vessel repair and rolling leukocytes in anti-TNF treated TNF-Tg mice that recovered lymphatic vessel contractions

WT and TNF-Tg mice (n=3) underwent TEM imaging as described in the Materials and Methods. Low magnification (2500×) imaging was used to identify lymphatic vessels, as shown in the representative WT (A). After identifying the lymphatic vessel, vessel walls were imaged at 10,000× magnification. Representative images from vessel walls are shown from: WT (B), untreated TNF-Tg with expanding PLN (C), untreated TNF-Tg with collapsed PLN (D), placebo (IgG) treated TNF-Tg with collapsed PLN (E), anti-TNF treated TNF-Tg with collapsed PLN (F). Highlighted in the images are the lumen (L), endothelial cells (EC) and smooth muscle cells (SMC). Note the absence of cells in the lumen in WT (B), the activated macrophage (Mϕ) with initial pseudopod attachment to EC afferent to expanded PLN (C), complete Mϕ attachment to EC afferent to collapsed PLN (D), exacerbated destruction of the lymphatic vessel in placebo treated mice as evidenced by vacuole formation in EC (red arrows in (E), mononucleated leukocytes that appear to be rolling along the endothelium in the anti-TNF treated TNF-Tg mice (red asterisks in F) indicative of restored cellular egress.

Table 1

Anti-TNF therapy increases monocyte and granulocyte numbers in lymph nodes efferent to arthritic joints in TNF-Tg mice

PLN from the TNF-Tg mice described in Figure 1 were harvested after 6-weeks of treatment, and analyzed by flow cytometry to quantify cells per PLN, which are presented as the mean ± SEM $\times 10^6$ cells per PLN (* $p<0.05$ by unpaired t-test).

	IgG treated	Anti-TNF treated	p-value
B cells ($CD19^+$)	1.4 ± 0.3	2.4 ± 0.8	n.s.
T cells ($CD3^+$)	0.5 ± 0.09	2.0 ± 0.7	n.s.
non-B/non-T ($CD19^-$, $CD3^-$)	1.8 ± 0.3	5.2 ± 1.0	0.009
monocytes/macrophages ($CD3^-$, $CD19^-$, $CD11b^+$, $CD11c^-$, $F4/80^+$)	0.8 ± 0.1	1.7 ± 0.4	0.047
granulocytes ($CD3^-$, $CD19^-$, $CD11b^+$, $CD11c^-$, $F4/80^-$, $Gr1^+$)	0.7 ± 0.09	2.0 ± 0.05	0.024